Extended quantum anomalous Hall effect in moiré structures: Phase transitions and transport

Adarsh S. Patri, Zhihuan Dong, and T. Senthil
Department of Physics, Massachusetts Institute of Technology, Cambridge, Massachusetts 02139, USA

(Received 24 September 2024; revised 14 November 2024; accepted 18 November 2024; published 6 December 2024)

Recent experiments on multilayer rhombohedral graphene have unearthed a number of interesting phenomena in the regime where integer and fractional quantum anomalous Hall phenomena were previously reported. Specifically, at low temperature (T) and low applied currents, an "extended" integer quantum anomalous Hall (EIQAH) state is seen over a wide range of the phase diagram. As the current is increased, at low T, the EIQAH state undergoes a phase transition to a metallic state at generic fillings, and to the fractional quantum anomalous Hall (FQAH) state at the Jain fillings. Increasing temperature at the Jain fillings also leads to an evolution out of the EIQAH state to the Jain state. Here we provide an interpretation of many of these observations. We describe the EIQAH state as a crystalline state (either of holes doped into the $\nu = 1$ state or an anomalous Hall crystal of electrons) that breaks moiré translation symmetry. At generic fillings, we show how an electric current-induced depinning transition of the crystalline order leads to peculiar nonlinear current-voltage curves consistent with the experiment. At Jain fillings, we propose that the depinning transition is preempted by an equilibrium transition between EIQAH and Jain FQAH states. This transition occurs due to the large polarizability of the Jain FQAH states, which enables them to effectively lower their energy in an applied electric field compared to the crystal states. We also discuss the finite-temperature evolution in terms of the relative entropies of the crystalline and FQAH states.

DOI: 10.1103/PhysRevB.110.245115

I. INTRODUCTION

Shortly after the discovery [1,2] of correlated electron physics in twisted bilayer graphene, it became clear [3–12] that many moiré materials will have nearly flat bands with Chern number making them ideal platforms to display ferromagnetism and integer/fractional quantum anomalous Hall (IQAH/FQAH) effects. The integer effect, and the associated ferromagnetism, were first observed [13–15] in a few graphene-based moiré systems, as well as in some transition-metal dichalcogenide (TMD) moiré systems [16,17]. Very recently, both the integer and fractional quantum anomalous Hall effects were observed [18–21] in twisted $MoTe_2$ and in pentalayer rhombohedral graphene [22] nearly aligned with a hexagonal boron nitride substrate (denoted R5G/hBN).

The standard mechanism [3,5,6,23] for the quantum anomalous Hall phenomena in moiré materials involves the following ingredients: First, the band structure is such that the bands in each valley have equal and opposite non-zero Chern number. Second, the valley (and spin, if present as an independent degree of freedom) polarizes into a ferromagnet due to interactions, thereby breaking time reversal spontaneously. If the electron filling is such that some bands, with a net nonzero Chern number, of the single occupied valley are fully filled, then an integer quantum anomalous Hall effect results. If the topmost band is partially filled, a fractional quantum anomalous Hall effect may be seen.

This standard mechanism accounts for the observed IQAH state in many moiré materials as well as the FQAH state in $t MoTe_2$. Remarkably, however, it fails in R5G/hBN, which makes this system particularly interesting. In R5G/hBN, the IQAH state is seen [22] in the conduction band when the electrons are at a total filling $\nu = 1$. Further, the effect is seen only in a large displacement field which drives the conduction electrons away from the aligned hBN layer. In these circumstances, the noninteracting band structure of R5G/hBN is such that, even when a single valley/spin flavor is occupied, there is no band gap at filling $\nu = 1$; rather, a metallic state results [24–26]. This is a result of the preferential occupation of the electrons in the layers furthest away from the aligned hBN which weakens the moiré potential. The opening of the band gap and the emergence of a Chern number are driven by Coulomb interactions, as demonstrated in Hartree-Fock calculations of the band structure [24–26]. Thus, even the IQAH state in R5G/hBN is the result of fascinating many-body physics. Further, upon rigidly doping the Hartree-Fock band (a crude approximation) at $\nu = 1$, numerical calculations [24–26] find FQAH states at $\nu = 2/3$ and other fillings, in broad agreement with experiments. Other similar n-layer rhombohedral graphene structures (RnG/hBN with $n = 4, 6, 7$) were argued [24–26] to display similar physics, but at different displacement field strengths. IQAH and FQAH states have since been seen in R4G/hBN [27] and R6G/hBN [28]. Various refinements [29–31] of this basic theoretical picture have been explored.

As emphasized in Refs. [25,26] (see, also, Ref. [24]), the Hartree-Fock calculations yield a band gap with a filled Chern band even if the moiré potential is completely turned off. The resulting state breaks continuous translation symmetry, and hence is denoted an "anomalous Hall crystal" (AHC). The stability of the AHC in the Hartree-Fock calculation has been explained through simplified models [32,33]. Whether such a state is really realized in R5G or whether a weak moiré potential is needed to enable it to occur is not currently

clear [33]. For further theoretical work on anomalous Hall crystals, see Refs. [34,35].

Very recent experimental results [27] on RnG/hBN show a very interesting phase diagram as a function of displacement field D, electron density measured through the moiré filling ν, the current bias I, and temperature T. At $\nu = 1$, the IQAH state reported earlier is reproduced. However, at $\frac{1}{2} < \nu < 1$, and at small I and T, in a tilted stripe region in the (D, ν) plane, there is an "extended" IQAH (EIQAH) state. A somewhat similar observation of an IQAH state was reported in Ref. [36], but just near $\nu = \frac{2}{3}$. For the EIQAH state of Ref. [27], when I is increased at low T, there is a transition either to a metallic state (at generic ν) or to the FQAH state reported earlier (at the Jain fillings). Further, upon increasing the temperature T at low I at the Jain fillings, the EIQAH phase reverts to the FQAH phase. Similar results are also found [27] in four-layer rhombohedral graphene on hBN (R4G/hBN).

At generic fillings, the longitudinal differential resistance as a function of I has an unusual shape: it is zero at low I (as expected) and has a sharp peak at the critical current before settling to a finite value at large I. This shape is suggestive of some kind of depinning transition, though it is seen in the resistance rather than the conductance. Interestingly, the low-T critical current for the EIQAH state is smaller [27] at the Jain fillings than at generic fillings, despite the possibility of commensuration effects strengthening any pinning processes in the former.

The purpose of this paper is to develop an explanation of these facts based on our current theoretical understanding of RnG/hBN. At first sight, it is tempting to interpret the EIQAH state in terms of an AHC that is stabilized in a range of filling, and we will explore this below. However, a less exotic state is one where holes doped into the $\nu = 1$ state localize by forming a crystal that is pinned either by impurities or (at commensurate fillings) by the moiré potential itself. We will show that such a hole crystal provides a natural explanation of many of the observations of Ref. [27] (and, to a large extent, so does the AHC).

The AHC may be thought of as a crystal formed by the electrons (counting from neutrality) with a period set by the electron density. In contrast, the hole crystal will have a period set by the hole density. We will argue that the electron and hole crystals are generically different and thus the two explanations are distinct. Thus, based on what is known so far, it is not possible to unambiguously advocate either for or against the AHC scenario for the EIQAH state. However, we present some (admittedly not very strong) arguments that suggest that the hole crystal may, in fact, be what is actually realized.

Our work clarifies the precise sense in which the observed current-voltage characteristics at generic filling are the result of depinning phenomena. In particular we show that due to the presence of a Hall component, the measured differential longitudinal resistance is proportional to the differential longitudinal conductance of the crystal without the Hall component. This leads to an understanding of the qualitative shape of the observed current-voltage curves. For the Jain fillings however, we propose that the depinning transition out of the EIQAH state is preempted by an equilibrium phase transition between crystal and FQAH states, and we present arguments for why the Jain state is favored by the current.

The remainder of the paper is organized as follows. In Sec. II, we describe the two possible classes of crystalline states that are pertinent to the EIQAH state: hole crystal and anomalous Hall crystal. In Sec. III, we discuss the transport signatures of the depinning transition of the hole crystal (at incommensurate fillings) and the field-induced EIQAH-FQAH transition at Jain fillings of the hole crystal. In Sec. IV, we discuss the transport and phase transitions from the perspective of the anomalous Hall crystal. In Sec. V, we consider the finite-temperature transitions between the EIQAH and FQAH states (at the Jain fillings) and discuss the possibility of an explanation in terms of the higher entropy of the FQAH state. Finally, we conclude in Sec. VI and provide some future directions of exploration.

II. EXTENDED INTEGER QUANTUM ANOMALOUS HALL REGION

We begin with some simple general considerations on the EIQAH state at fillings $\frac{1}{2} < \nu < 1$. Generically, for any $\nu < 1$, the partial filling of the moiré unit cell will naturally break the moiré translation symmetry unless there is either fractionalization and the associated topological order or there are gapless charge excitations. The former happens in, e.g., the FQAH state and the latter happens in, e.g., a Fermi-liquid metal. Clearly, the EIQAH state is not metallic and has integer Hall conductance. While exotic gapped states without any fractional Hall conductivity are possible [37] at fractional rational filling, we will be content to explore the simpler and more likely possibility that the EIQAH state breaks moiré translation symmetry. With this assumption, there still are two possible classes of crystalline states [38]:

(i) *Hole crystal.* The first possibility is a [Wigner or charge density wave (CDW)] crystal of holes forming on top of the $\nu = 1$ state at a hole filling of $\nu_h = 1 - \nu$. This hole crystal (henceforth referred to as CDW) has its period set by ν_h. At a generic ν_h, this crystal will be pinned by impurities in the device. At commensurate fillings, it will lock to the moiré lattice. Note that the holes not only observe the bare moiré potential, but also the self-consistently generated electronic potential from the many-body state at $\nu = 1$. Thus the effective periodic potential seen at the moiré period will be enhanced over the bare moiré potential, and we expect the locking to be strong. An example of a commensurate hole crystal at $\nu = 2/3$ (i.e., $\nu_h = 1/3$) is shown in Fig. 1: the hole crystal forms a triangular lattice, where the charge density resides on select sites of the moiré unit cell and gains commensuration energy from the underlying moiré potential. For other rational fillings $\nu = 3/5$ (i.e., $\nu_h = 2/5$), the hole crystal may not necessarily be a triangular lattice, but instead may be determined by the Coulomb interactions on the lattice.

(ii) *Anomalous Hall crystal.* The second possibility is that of an anomalous Hall crystal $(\text{AHC})_\rho$ which is formed by electrons at filling ν. Here the subscript denotes that the period of the electronic crystalline state is determined by the electronic density. Clearly, this state also breaks moiré translation symmetry for any $\nu \neq 1$. However, the electrons

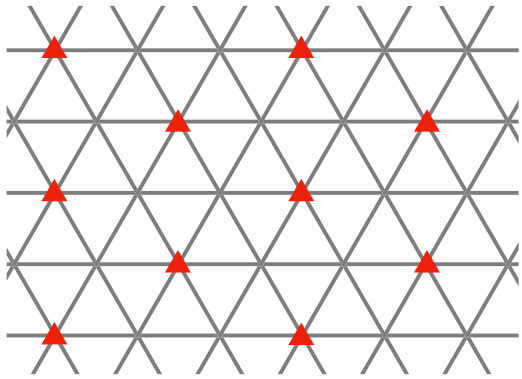

FIG. 1. Hole crystal forming on top of IQAH state at rational fillings of the moiré unit cell. Here, a hole crystal is depicted for $\nu = 2/3$. The holes shown by red triangles (of filling $\nu_h = 1/3$) can form a triangular lattice, which locks to the moiré lattice.

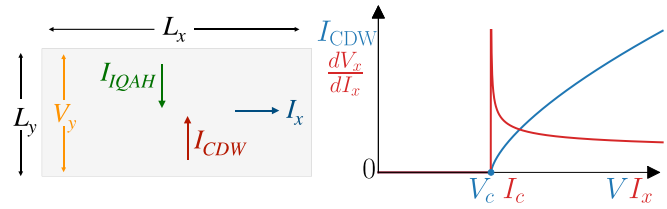

FIG. 2. Depinning transition of hole crystal (CDW). Left: Schematic of sample illustrating the interplay of the CDW and IQAH component at the hole-crystal depinning transition, where a counterpropagating I_{IQAH} current cancels the I_{CDW} sliding current. In actuality, the CDW component slides at an angle θ_H with respect to the $\hat{x}$ direction, with the generated IQAH current component in the direction perpendicular to the CDW current direction to yield a net current flowing along I_x. Right: CDW current (blue) as a function of Hall voltage and differential resistance (red) as a respective function of Hall voltage (V) and bias current (I_x) depicting the depinning transition for critical exponent $\beta = 2/3$.

forming this state see only the weak bare moiré potential. Thus, we expect it can be essentially described as the $(\mathrm{AHC})_\rho$ of the continuum system that is only weakly perturbed by the moiré potential. The crystal structure of $(\mathrm{AHC})_\rho$ will hence be triangular, and such that each unit cell of this triangular lattice has one electron. It is easy to see that the fillings at which this triangular lattice is commensurate—and, in the process, gain some commensuration energy—with the moiré lattice are $\nu = (n^2 + m^2 + nm)^{-1}$, where $n, m \in \mathbb{Z}$ [39]. This entails that the only fillings where the $(\mathrm{AHC})_\rho$ is commensurate with the moiré lattice are either at $\nu = 1$ or at $\nu \leqslant 1/3$. Thus, in the range of interest, $\frac{1}{2} < \nu < 1$, the $(\mathrm{AHC})_\rho$ is an incommensurate triangular lattice that "floats" on top of the moiré lattice. It will only be pinned by impurities.

The crystal states we are concerned with in this paper should be distinguished from the "parent" (possibly moiré-enabled [33]) anomalous Hall crystal discussed for the $\nu = 1$ state itself. This parent crystal has a period set by the moiré lattice spacing. At $\nu = 1$, this crystal period is the same as the period set by the electron density, but is different at other ν. To emphasize this, we denote this parent crystal as $(\mathrm{AHC})_M$. If such a parent crystal forms at $\nu \neq 1$, there will inevitably be extra holes or electrons to make up the right density. These will then form many-body states of their own. Thus, the IQAH component of the hole-crystal state envisaged above should be viewed as $(\mathrm{AHC})_M$. Similarly, the FQAH states (at least for $\nu > 1/2$) are most usefully discussed in the hole picture, and hence thought of as a combination of $(\mathrm{AHC})_M$ and an FQAH state of holes. Beyond setting the stage for these many-body states to form at $\nu \neq 1$, the $(\mathrm{AHC})_M$ does not play a direct major role in this paper, and hence we will not discuss it further.

At $\nu \neq 1$ and low current bias, either the hole or electron crystals discussed above will stay pinned, due either to impurities or to commensuration or both, and will have an integer quantum anomalous Hall effect. We identify these with the EIQAH state seen in experiments. In the following, we analyze their properties in more detail, focusing on the depinning phenomenon at generic filling and their transition to FQAH states at the Jain fillings.

III. TRANSPORT AND PHASE TRANSITIONS OF THE HOLE CRYSTAL

In this section, we focus on the hole crystal and discuss the transition out of this state induced upon increasing the electric current.

A. Depinning transition at incommensurate fillings

At incommensurate fillings, the many-body state can be imagined as being segmented into an integer quantum anomalous Hall component ($\nu = 1$) and a hole crystal (ν_h). We consider running a current I_x along the $\hat{x}$ direction in a sample of dimensions $L_x \times L_y$, as depicted in Fig. 2. The sample geometry is such that leads are connected in the $\hat{x}$ direction with an open circuit in the $\hat{y}$ direction. The hole crystal, as discussed in Sec. II, is pinned by the disorder (at low currents). Then the current is carried by the IQAH component, which leads to a Hall voltage, $V_y = \frac{h}{e^2} I_x$. The corresponding electric field is felt by the hole crystal. As is well known, a pinned crystal will, when subject to a large enough electric field, start sliding. The evolution to the sliding state at $T = 0$ happens through a sharp dynamical phase transition. We discuss below the subsequent longitudinal differential resistance.

We first give a simplified treatment that captures the essential physics. As the electric field is along $\hat{y}$, the crystal component will slide along $\hat{y}$. (Here we are ignoring any anomalous velocity of the sliding hole crystal.) Just above the threshold electric field, the sliding crystal will thus lead to a small electric current $I_{y,\mathrm{CDW}}$ along the $\hat{y}$ direction, which must be canceled by an equal and opposite current $I_{y,\mathrm{IQAH}} = -I_{y,\mathrm{CDW}}$ from the IQAH component due to the open circuit along $\hat{y}$. In turn, $I_{y,\mathrm{IQAH}}$ generates a voltage along $\hat{x}$,

$$V_x(I_x) = -\frac{h}{e^2} I_{y,\mathrm{IQAH}} = \frac{h}{e^2} I_{y,\mathrm{CDW}}\left(V_y = \frac{h}{e^2} I_x\right), \qquad (1)$$

where the minus sign in the first equality is due to the direction of the current flow, and in the last equality we have used the aforedescribed Hall relation. We thus arrive at the differential

(longitudinal) resistance,

$$\frac{dV_x}{dI_x} = \left(\frac{h}{e^2}\right)^2 \frac{dI_{y,\mathrm{CDW}}(V)}{dV}\bigg|_{V=\frac{h}{e^2}I_x}. \tag{2}$$

Strikingly, the differential resistance of the combined IQAH state and hole-crystal state is proportional to the differential conductance of the hole crystal.

The depinning behavior near threshold of an incommensurate crystal is an old and much studied problem in statistical mechanics. For reviews, see Refs. [40–43]. The details depend on whether the sliding is in the elastic regime or in a plastic regime (where topological defects of the ordering pattern are nucleated), whether the interactions are short range or long range, and the pattern of charge ordering. It is expected that for weak disorder, plastic deformations of the crystal may be ignored (except perhaps at very long length scales [41–43]). In that case, near the threshold, $I_{\mathrm{CDW}}(V > V_c) \sim (V - V_c)^\beta$, where $\beta < 1$ [43].

This can lead to a singular peak in the differential resistance (for $\beta < 1$), as shown in Fig. 2, in agreement with the experimental observation of the sharp transition feature at generic fillings. The combination of the depinning of the hole crystal in conjunction with the interplay with the IQAH component leads to this feature.

The above treatment, though capturing the essentials of the interplay of the hole-crystal and IQAH components, ignored the sliding of the hole crystal along the $\hat{x}$ direction by the Hall voltage V_x. We define the electric field components $E_{x,y} = V_{x,y}/L_{x,y}$, where $V_{x,y}$ are the voltage drops along the $\hat{x}, \hat{y}$ directions, and the corresponding current densities $J_{x,y} = I_{x,y}/L_{x,y}$. The total current density is composed of the IQAH and CDW components, $\vec{J} = \vec{J}_{\mathrm{CDW}} + \vec{J}_{\mathrm{IQAH}}$, such that $J_y = 0$ due to the open circuit in the $\hat{y}$ direction. The net electric field is generated by the IQAH component and is thus perpendicular to the total $\vec{J}^{\mathrm{IQAH}}$, i.e., $\vec{E} = \frac{h}{e^2}\hat{z} \times \vec{J}_{\mathrm{IQAH}}$, where $\vec{J}_{\mathrm{IQAH}}$ is the current density associated with the IQAH component. When the CDW component slides, there will be a current along the electric field direction [44]: $\vec{J}_{\mathrm{CDW}} \parallel \vec{E}$.

Defining the Hall angle θ_H (angle between total electric field and current) and projecting the total current J_x along and perpendicular to the direction of the electric field yields

$$|\vec{J}_{\mathrm{CDW}}| = J_{\mathrm{CDW}} = J_x \cos(\theta_H), \tag{3}$$

$$|\vec{J}_{\mathrm{IQAH}}| = J_{\mathrm{IQAH}} = J_x \sin(\theta_H). \tag{4}$$

The incommensurate hole crystal will have a nonlinear current-voltage relationship $J_{\mathrm{CDW}} = f(E)$, where the function f will be nonzero only beyond a sharp threshold value of its argument. Using $|\vec{E}| = \frac{h}{e^2}J_{\mathrm{IQAH}}$, we arrive at the self-consistent equation for the total current,

$$J_x \cos(\theta_H) = f\left[\frac{h}{e^2}J_x \sin(\theta_H)\right]. \tag{5}$$

Equation (5) permits the Hall angle to be extracted from the magnitude of the total current, $\theta_H = \theta_H(J_x)$.

For small currents, $f = 0$, which leads to $\theta_H = \frac{\pi}{2}$. For currents just above the depinning threshold, we take $f(E) \approx A(E - E_c)^\beta$, where E_c is the depinning electric field, $\beta < 1$ is the critical exponent defined above, and A is a constant. Since the critical current just above the threshold is small, we can assume $\theta_H \approx \pi/2 - \delta$, where δ is taken to be small. Expanding Eq. (5) in the small-δ limit yields $V_x = \tilde{A}(I_x - I_c)^\beta$, where $\tilde{A}$ is a constant. We thus arrive at the same singular form of the differential longitudinal resistivity as in the simplified treatment. Similarly, we can obtain the correction due to the sliding of the hole crystal to the Hall resistivity of $\sim[(h/e^2)J_x - x_c]^{2\beta-1}$.

B. Current-induced EIQAH-FQAH transition at Jain fillings

At the specific Jain fillings of the moiré unit cell, the current-driven transition from the IQAH state to the FQAH state occurs at a smaller critical current than at the generic incommensurate fillings. This is surprising because, as described in Sec. II, due to the enhanced role of the moiré potential at rational fillings, commensuration effects, and hence the depinning thresholds, are expected to be larger. Thus, we propose that the current-induced transition at the Jain fillings is not a depinning of the hole crystal, but rather is an equilibrium transition where the IQAH component is unchanged, while the ground state of the holes changes from the commensurate crystal to an FQAH state.

Consider the Jain FQAH state at filling $\nu = p/(2p+1)$, where for $\nu > 1/2$ this entails $p < 0$. This state can be regarded as the particle-hole conjugate of the Jain state of holes at filling $\nu_h = 1 - p/(2p+1) = (p+1)/(2p+1)$. This allows us to regard the FQAH state at the Jain fillings as an IQAH + hole-Jain state. For example, the $\nu = 2/3$ Jain state is equivalent to the IQAH + ($\nu_h = 1/3$) hole-Jain state; similarly, the $\nu = 3/5$ Jain state is equivalent to the IQAH + ($\nu_h = 2/5$) hole-Jain state. Thus, at low bias currents, the two competing many-body states at these fillings are (a) IQAH + hole-crystal and (b) IQAH + hole-Jain states. It is important to reiterate that the $\nu = 1$ IQAH state is the same in both many-body states.

Since the current in a quantum Hall liquid is carried by its edge state (and has no dissipation), the many-body state at a nonzero current is an equilibrium state [45] and we can ask about its ground-state energy. Thus our proposal is that the depinning transition at incommensurate fillings is preempted at the Jain fillings by the transition to the Jain FQAH states.

The transition between a hole-crystal and hole-Jain state may occur under the tuning of external knobs, such as displacement field, even at zero-bias current. This transition may even be allowed to be continuous [46], but here we will consider the more conventional possibility that it is a first-order transition. Let g be a parameter (e.g., a displacement field) that tunes across this first-order transition at $T = I = 0$. At the transition point $g = g_c$, the ground-state energy per hole is equal between the two states, $E_{\mathrm{CDW}}(g = g_c) = E_{\text{hole-Jain}}(g = g_c)$. For $g < g_c$ (the evident state of the experimental sample at lowest temperatures), $E_{\mathrm{CDW}}(g < g_c) < E_{\text{hole-Jain}}(g < g_c)$. Nonetheless, we expect the two energies (per hole) to be close to each other, as is known from the competition between crystal and liquid states in standard Landau levels, as well

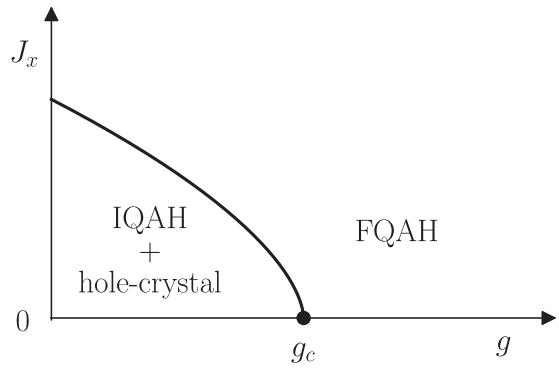

FIG. 3. Schematic of the current- (J_x) induced phase transition from IQAH + hole-crystal to FQAH state. g denotes a parameter that tunes across a first-order transition at $T = I = 0$. The first-order phase boundary bends towards the IQAH + hole-crystal state, indicative of the enhanced dielectric susceptibility of the Jain states.

as other contexts (see, e.g., the discussion in Ref. [33], and references therein).

We now consider the relative stability of the hole-crystal and hole-Jain states in the presence of an electric current, $\vec{J} = J_x\hat{x}$. The induced Hall electric field will lead to an electric polarization which will lower the energy of either state and will affect their relative stability, as we discuss below. We provide a schematic phase diagram of the current-induced phase transition from the IQAH + hole-crystal to FQAH state in Fig. 3.

1. IQAH + hole-crystal state

The IQAH background component is the sole carrier of the current, which gives rise to a perpendicular Hall electric field $E_y = \frac{h}{e^2}J_x$. Since the applied bias current is smaller than the depinning threshold current, the hole crystal does not slide, but instead develops an electric polarization. The modification of the ground-state energy due to this polarization will (for small currents) be

$$E_{\text{CDW}}(J_x) = E_{\text{CDW}}(J_x = 0) - \frac{\chi_{\text{CDW}}}{2}\left(\frac{h}{e}\right)^2 J_x^2, \tag{6}$$

where χ_{CDW} is the dielectric susceptibility of the hole crystal. We expect χ_{CDW} to be a smooth function of the filling ν.

2. IQAH + hole-Jain state

For the IQAH + hole-Jain state, the current (and, consequently, conductivity) is composed of the contribution from both IQAH and the hole-Jain components,

$$\begin{aligned}\sigma_{xy} &= \sigma_{xy}^{\text{IQAH}} + \sigma_{xy}^{\text{hole-Jain}} \\ &= \frac{e^2}{h} - \frac{e^2}{h}\frac{p+1}{2p+1} \\ &= \frac{e^2}{h}\frac{p}{2p+1},\end{aligned} \tag{7}$$

where the negative sign in the second line is due to the hole charge. We thus obtain the corresponding electric field, $E_y = \frac{h}{e^2}\frac{2p+1}{p}J_x$. The hole-Jain state will also develop an electric polarization due to this Hall electric field,

$$\begin{aligned}E_{\text{hole-Jain}}(J_x) &= E_{\text{hole-Jain}}(J_x = 0) \\ &- \frac{\chi_{\text{hole-Jain}}}{2}\left(\frac{h}{e}\right)^2\left(\frac{2p+1}{p}\right)^2 J_x^2,\end{aligned} \tag{8}$$

where $\chi_{\text{hole-Jain}}$ is the corresponding dielectric susceptibility. For large $|p|$ (i.e., fillings closer to $\nu = 1/2$), the electric field responsible for the polarization of the hole-Jain state is two times larger than the electric field polarizing the hole crystal due to the reduced Hall conductivity.

Unlike the hole crystal's dielectric susceptibility, the dielectric susceptibility of the Jain state will grow with increasing $|p|$, and eventually diverge. Thus the hole-Jain state for large $|p|$ can lower its energy in the presence of a current more effectively than the hole crystal can. It then follows that for $g < g_c$, there will be a transition at a nonzero current where the ground state flips from the EIQAH to FQAH states. To understand the Jain state's susceptibility, first recall that the termination of the Jain series as $|p| \to \infty$ is the $\nu = 1/2$ compressible composite Fermi liquid (CFL) where the static wave-vector-dependent dielectric function $\chi(q) = \frac{\kappa}{q^2}$ for small q (here, κ is the electronic compressibility). If the electron density changes by $\delta\rho$ to move away from $\nu = 1/2$, the composite fermions see an effective magnetic field $B^* = -4\pi\delta\rho$. There is a corresponding length scale ${l_{B^*}}^2 = \frac{1}{B^*}$. The small-$q$ divergence of $\chi(q)$ will be cut off at a momentum scale $\frac{1}{{l_{B^*}}^2} = B^*$, leading to a dielectric susceptibility,

$$\chi_{\text{hole-Jain}} = \kappa l_{B^*}^2 \sim |p|, \tag{9}$$

where we have employed the fact that $|B^*| = B/(2p+1)$ at the Jain fillings. Thus, as promised, for Jain fillings close to $\nu = 1/2$ (i.e., large $|p|$), the dielectric susceptibility is very large. This ensures that the hole-Jain state will always be stabilized by a small J_x over the hole crystal for Jain fillings sufficiently close to $\nu = 1/2$. A detailed energy comparison away from this asymptotic limit ultimately requires an accurate model for the hole-crystal and hole-Jain states, and is beyond the purview of our study. We demonstrate, in Appendix A, a mean-field composite fermion treatment for the energy decrease of the Jain state, which confirms the above-presented argument. We emphasize that the above argument for the dielectric susceptibility is beyond the mean-field treatment.

IV. TRANSPORT AND PHASE TRANSITIONS OF THE ANOMALOUS HALL CRYSTAL

Next we turn to the $(\text{AHC})_\rho$ state, which is an electron crystal (with a period determined by the charge density) and whose occupied bands have nonzero Chern number $C = 1$. At low current strengths $\vec{J} = J_x\hat{x}$, the $(\text{AHC})_\rho$ will stay pinned by impurities. The nonzero Chern number leads to a Hall electric field, $E_y = \frac{h}{e^2}J_x$. With increasing current, this electric field will also increase and, like in any other pinned crystal, will eventually lead to a sharp depinning transition at $T = 0$. Beyond the threshold, the AHC will slide, but now in a direction that is different from that of the electric field. This is because the sliding AHC will have an anomalous velocity (just like it does in the pinned state). We analyze the transport properties across the depinning transition below and show that

it will have the same qualitative behavior as the incommensurate hole crystal (and the experiments). Subsequently, we will discuss the situation at the Jain fillings.

1. Depinning transition of anomalous Hall crystal (AHC)$_\rho$

Consider the current response of the (AHC)$_\rho$ to an electric field $\vec{E}$. In general, we can write this as

$$\vec{J} = \sigma_{xx}(E)\vec{E} + \sigma_{xy}(E)\vec{z} \times \vec{E}. \tag{10}$$

Here, σ_{xx}, σ_{xy} are the (nonlinear) longitudinal and Hall conductivities (*not* the differential conductivities) that are functions of $E = |\vec{E}|$. For E below some threshold E_T, we have

$$\sigma_{xx}(E < E_T) = 0; \;\; \sigma_{xy}(E) = \frac{e^2}{h}. \tag{11}$$

What happens beyond the threshold? We expect that the longitudinal current is similar to an ordinary sliding crystal. We therefore focus on the anomalous (i.e., Hall) current. To understand this, consider a sliding AHC in the complete absence of any impurity pinning which is appropriate deep into the sliding phase. In this limit, we can use a semiclassical framework for the many-particle system to obtain an effective equation of motion for the center-of-mass motion. This is detailed in Appendix B. We find an anomalous center-of-mass velocity,

$$\langle \vec{v}_{\rm CM} \rangle = \vec{E} \times \hat{z} \left\langle \int \frac{d^2\vec{p}}{(2\pi)^2} \mathcal{B}_\alpha(\vec{p}) c^\dagger_{\alpha\vec{p}} c_{\alpha\vec{p}} \right\rangle, \tag{12}$$

where $\mathcal{B}_\alpha(\vec{p})$ is the microscopic Berry curvature of a microscopic electron of flavor α with corresponding fermionic operators c. The average is evaluated in the many-body state (for vanishing electric field, $\vec{E} = 0$). We computed this averaged Berry curvature within Hartree-Fock theory for R5G/hBN; it lies in the range ≈1–50 for displacement field energies u_d ranging from 10 to 50 meV at a range of twist angles $\theta \in [0^\circ, 1.5^\circ]$. The center-of-mass anomalous velocity of the AHC determines the Hall current $\vec{J}_{\rm Hall} = \rho \langle \vec{v}_{\rm CM} \rangle$, where ρ is the charge density. The crucial point is that $\sigma_{xy}(E \gg E_T) = \rho \neq 0$, but is also not quantized. Across the continuous dynamical transition at E_T, we expect that $\sigma_{xy}(E)$ will evolve continuously from its quantized value for $E < E_T$ to its unquantized value for $E \gg E_T$. However, we will not attempt to describe the details of the critical behavior of the anomalous velocity near the threshold. Once we accept that $\sigma_{xy}(E \approx E_T)$ is close (or exactly equal) to e^2/h, the analysis of the longitudinal differential resistivity becomes identical to that in Sec. III for the incommensurate hole crystal. Thus there will be a peak in the longitudinal differential resistance at low E, and pass through a peak at the threshold, before settling to a finite nonzero value in the sliding phase.

Thus we see that the (AHC)$_\rho$ possesses both a longitudinal conductivity qualitatively similar to the incommensurate hole crystal. The distinction with the IQAH + hole-crystal picture is that here the (AHC)$_\rho$ contains both longitudinal and Hall components in one electronic entity.

The detailed behavior of the Hall component near the threshold is an interesting theoretical problem for the future.

2. Current-induced transition to Jain FQAH state

The discussion on the current-induced transition from the hole-crystal to the Jain FQAH state can be taken over without any modification to the (AHC)$_\rho$ as well, and we will mainly highlight some differences. In short, we propose that the depinning transition of the (AHC)$_\rho$ is preempted by a current-induced first-order transition to the Jain FQAH state. In the presence of a current J_x, the pinned (AHC)$_\rho$ will experience the Hall electric field and will develop a polarization that lowers its energy of $O(J_x^2)$. The coefficient is proportional to the dielectric susceptibility, which will be a smooth nondiverging function of ν. Thus the large susceptibility of the Jain FQAH state can help stabilize it over the (AHC)$_\rho$, as detailed in the discussion on the hole crystal.

However, we find this proposal somewhat less compelling in the (AHC)$_\rho$ than in the hole crystal. As we emphasize below, in the latter, the effect of the moiré potential is expected to be enhanced, and hence the depinning thresholds at the Jain fillings may be large enough that they can be preempted by the transition to the FQAH state. In contrast, in the (AHC)$_\rho$, there is nothing special about the Jain fillings as far as pinning thresholds go. They are expected to evolve smoothly across these fillings. It is then not clear that the depinning transition can be preempted in the manner described in the previous paragraph. A second concern is that while the hole-crystal and the Jain states can reasonably be expected to have a close competition (i.e., have close energies/particle) even away from the first-order transition point, this is less clear for the (AHC)$_\rho$ and the Jain states. These two states are rather different from each other and any closeness of their energies may be specific to a narrow region near their presumed first-order transition.

V. FINITE-TEMPERATURE TRANSITIONS BETWEEN EIQAH AND FQAH STATES AT THE JAIN FILLINGS

The EIQAH state is stabilized at the base temperature [27] (∼10 mK). As the temperature rises to $T_c \sim 100$ mK, a transition from EIQAH to FQAH states is observed for the Jain fillings $\nu = \frac{2}{3}, \frac{3}{5}$. It is possible that this phenomenon has a mundane explanation due to experimental artifacts such as equilibration issues between the contacts and the edge modes at low T [47]. Here, however, we will explore the possibility of an explanation where such a transition is an intrinsic bulk phenomenon. Then the experimental observation suggests that the FQAH state is slightly higher in energy than the EIQAH state, but it also has higher entropy, which at higher temperatures reduces its free energy.

Certainly, this entropy difference should be attributed to low-energy excitations. The pertinent excitations are those at an energy scale that is lower or at least similar to the transition temperature $T_c \sim 100$ mK ~ 0.01 meV, so that they contribute significant entropy at T_c. Candidate excitations are charged quasiparticles or neutral collective modes. The charged gap of the hole-crystal and the (AHC)$_\rho$ state should be of the order of the Coulomb repulsion. For the FQAH state, at least close to $\nu = 1/2$, the charge gap will become small (order $\frac{1}{|p|}$ in composite fermion mean-field theory). Away from this limit, the gaps are not accurately known, but we can take guidance from existing calculations. According to

numerics, within the approximation that the interaction-induced Chern band is treated as frozen, the FQAH state at $\nu = \frac{2}{3}, \frac{3}{5}$ has a gap of $\sim$1 meV [24–26]. The most important neutral modes are the phonons of the broken translation symmetry. At Jain fillings, there are three competing states: (1) electron-crystal $(\mathrm{AHC})_\rho$, (2) IQAH + hole-crystal, and (3) IQAH + hole-Jain states. In (2) and (3), the IQAH component really is $(\mathrm{AHC})_M$. In the absence of a moiré potential, all of these break continuous translation symmetry and therefore have gapless phonons. In the presence of a moiré potential, a phonon gap is opened of size determined by the effective moiré potential strength. Note, in particular, the enhancement of the moiré potential by the underlying IQAH state for (2). However, the phonon for (1) remains gapless since the $(\mathrm{AHC})_\rho$ lattice is incommensurate with the moiré lattice.

Armed with this understanding, we can discuss the finite-T evolution of the EIQAH phase. Due to its gapless phonon, the $(\mathrm{AHC})_\rho$ will have a high entropy at low T compared to the other two states. Thus, if it is already the preferred ground state, it is unlikely to yield to the FQAH state on the scale of 100 mK. However, in the experiment, the EIQAH transitions into FQAH state at higher temperatures. This suggests that the underlying low-temperature EIQAH state is more likely to be the IQAH + hole-crystal state, as it does not manifestly overwhelm the FQAH state at higher temperatures, unlike the $(\mathrm{AHC})_\rho$ state. The high-temperature stabilization of the FQAH state relative to the hole crystal is easy to understand for ν close to $1/2$, where the charged excitations of the former have increasingly small gaps. Well away from $\nu = 1/2$, based on the estimates above, the charged excitations are unlikely to play a role at the 10 mK scale. Evaluation of the relative stability of the hole-crystal and FQAH states at nonzero T will have to await a better understanding of the excitation spectrum of either state.

VI. DISCUSSION

In this work, we examined the nature of the extended integer quantum anomalous Hall (EIQAH) phase [27,36] realized at low bias currents and temperatures in rhombohedral graphene moiré structures. For very general theoretical reasons, the EIQAH state away from $\nu = 1$ breaks moiré translation symmetry. Thus the main question is the nature of the resulting crystalline state, its depinning transition, and its competition with the FQAH state at Jain fillings. We explored two possible crystalline states away from $\nu = 1$: (a) a crystal of holes doped into the $\nu = 1$ state (IQAH + hole-crystal state) and (b) an electron crystal with a quantized anomalous Hall effect (in its pinned state), known as the anomalous Hall crystal $(\mathrm{AHC})_\rho$. The hole crystal experiences an enhanced moiré potential (due to the self-consistently generated electronic potential from the $\nu = 1$ background) which enhances the commensuration effects. In contrast, the natural $(\mathrm{AHC})_\rho$ state (with one electron per unit cell) is incommensurate for any filling $1/2 < \nu < 1$ where the EIQAH state is seen. Thus the moiré lattice is expected to play a more important role in the hole crystal compared to the $(\mathrm{AHC})_\rho$ crystal.

At generic fillings, either crystal is pinned by impurities. The current-induced transition out of the EIQAH state observed at generic fillings in the experiments [27] can be understood as a depinning of the crystal. For the IQAH + hole-crystal state, the interplay of the sliding hole-crystal and the IQAH component leads to a sharp peak in the differential resistance at threshold. In the $(\mathrm{AHC})_\rho$ picture, the threshold behavior can similarly be understood, with the only difference being that the Hall and longitudinal components are due to the same electrons.

At the Jain fillings, we proposed that the current-induced transition out of the EIQAH state is not a depinning transition of the crystal. Rather the depinning transition is preempted by a ground-state phase transition to the Jain FQAH state. For the hole crystal, it is natural to expect that it closely competes with the FQAH state (which can be viewed as a hole-Jain state) at the same filling. Thus even if the hole crystal wins at zero current, the energy balance can be tipped in an electric field depending on which of these states has a higher dielectric susceptibility. We analyzed this effect and showed that for fillings close to $\nu = 1/2$, the Jain state will have a strongly enhanced susceptibility (inherited from the proximity to the compressible composite Fermi liquid at $\nu = 1/2$). The hole crystal does not have any such enhancement and, hence, an external current (and the associated Hall electric field) can drive a transition from the hole-crystal to the Jain FQAH state. In principle, a similar picture may also apply to the competition between $(\mathrm{AHC})_\rho$ and the FQAH state. However, it is less clear if these states are close competitors.

Finally, we discussed the finite-temperature transition to the FQAH state in the framework of entropy gain of the FQAH states relative to the EIQAH state. We suggested that the pertinent excitations for the entropy may be phonon modes of the various crystals as they are likely to have lower energy than the charged excitations. Unlike the hole-crystal and the Jain FQAH state, the $(\mathrm{AHC})_\rho$, being incommensurate with moiré, will have an ungapped phonon spectrum even at the Jain fillings, and hence have a higher entropy than the FQAH state. This makes it harder to understand the stabilization of the FQAH state at higher temperatures if the $(\mathrm{AHC})_\rho$ is realized in the EIQAH state. The relative thermal stability of the IQAH hole-crystal and the FQAH states is hard to evaluate without a more detailed understanding of the excitation spectrum of either state than is currently available. Thus we do not have a good explanation of the finite-T evolution at present, and this is a target for future work.

We have only attempted to provide a "broad-brush" discussion of the basic physics of these crystalline states and their transitions, and we leave open many detailed questions for the future. First, it will be important to take a more microscopic approach in discussing the phase competition between crystal and FQAH states at the Jain fillings. Second, there are interesting questions associated with the depinning transition in the presence of the Hall component, including a detailed picture of the threshold behavior of the differential Hall conductance. Finally, our discussion of the entropy of the various competing states highlights the need for accurate microscopic studies of the excitations of these various competing states.

Note added. Recently, we learned of Ref. [48], which examines the thermal evolution from EIQAH to FQAH, and argues that the disorder plays an important role. In addition, Refs. [49,50] examine the thermal evolution from EIQAH to FQAH states from the perspective of edge entropy, and

Ref. [51] uses a toy model with impurities to examine the appearance of FQAH states at finite temperature.

ACKNOWLEDGMENTS

We thank L. Ju, T. Han, and Z. Lu for sharing and discussing their experimental data. We also thank P. Lee, M. Kardar, C. Marchetti, M. Yankowitz, A. Young, and Y.-H. Zhang for pertinent discussions. T.S. was supported by NSF Grant No. DMR-2206305, and partially through a Simons Investigator Award from the Simons Foundation. This work was also partly supported by the Simons Collaboration on Ultra-Quantum Matter, which is a grant from the Simons Foundation (Grant No. 651446, T.S.).

APPENDIX A: DIELECTRIC SUSCEPTIBILITY WITHIN MEAN-FIELD COMPOSITE FERMION THEORY

In this Appendix, we employ the composite fermion mean-field framework to calculate the dielectric susceptibility. We examine the Jain state at filling $\nu_h = \frac{p+1}{2p+1}$ as being constructed from occupying Landau levels with composite fermions. The effective low-energy Lagrangian is

$$\mathcal{L} = \frac{1}{2\pi} A \wedge db - \frac{2}{4\pi} b \wedge db - \frac{1}{2\pi} b \wedge da + \mathcal{L}[\psi_{\rm cf}, a], \tag{A1}$$

where A is the external background gauge field, a, b are the internal gauge fields, and $\mathcal{L}[\psi_{\rm cf}, a]$ is the Lagrangian involving the composite fermions and its respective gauge field a. The physical electric current carried by the holes along the $\hat{x}$ direction is

$$J_x^{\rm hole} = \frac{1}{2\pi} e_y^b = \frac{1}{2\pi}(-\partial_y b_0 - \partial_0 b_y). \tag{A2}$$

The total current $J_x = J_x^{\rm hole} + J_x^{\rm IQAH}$ can be related to the current carried by the holes via the background electric field E_y,

$$J_x^{\rm hole} = \frac{p+1}{p} J_x \Rightarrow \frac{e_y^b}{E_y} = \frac{p+1}{2p+1}. \tag{A3}$$

Varying the Lagrangian Eq. (A1) with respect to b in the presence of the external magnetic field along the $\hat{y}$ direction yields

$$e_y^a = E_y - 2e_y^b \tag{A4}$$

$$= -\frac{E_y}{2p+1}, \tag{A5}$$

where we have used that $dA = -E_y$ and similarly for the internal gauge fields, and in the second equality we employed Eq. (A5).

The composite fermions experience the electric field e_y^a. Within first quantization, the coupling of the electric field to the composite fermion location is $H_e = -y e_y^a$. Within Landau levels, $\langle H_e \rangle = 0$, indicating the lack of dipole moment in the ground states. The dielectric susceptibility is computed with second-order perturbation theory,

$$\frac{\Delta\epsilon}{N} = \sum_{m>n} \left(e_y^a\right)^2 \frac{|\langle m|y|n\rangle|^2}{-\hbar\omega_c^*(m-n)}, \tag{A6}$$

where ω_c^* is the cyclotron frequency associated with the effective magnetic field B^* experienced by the composite fermions. For Landau levels, only for $m = n+1$ is the matrix element nonvanishing (recall $m > n$ in the summation), and so

$$\frac{\Delta\epsilon}{N} = -\left(e_y^a\right)^2 \frac{m^*}{(B^*)^2} c \tag{A7}$$

$$= -E_y^2 |p| m^* c, \tag{A8}$$

where c is a numerical factor, and we have once again employed Eq. (A5) for e_y^a. It follows that the dielectric susceptibility is

$$\chi_{\text{hole-Jain}} \sim |p| m^*. \tag{A9}$$

Assuming the effective mass stays constant as $|p| \to \infty$, then dielectric susceptibility diverges as $\nu \to 1/2$. Thus the Jain state will always be stabilized by a small current J_x for sufficiently large $|p|$, i.e., for fillings sufficiently close to $1/2$.

APPENDIX B: ANOMALOUS DRIFT VELOCITY WITHIN SEMICLASSICAL FRAMEWORK

In this Appendix, we derive the anomalous drift velocity of the $(\text{AHC})_\rho$ within a semiclassical framework. Consider the microscopic semiclassical equations of motion for an electron of the continuum rhombohedral-stacked n-layer graphene (RnG) Hamiltonian,

$$H = \sum_i \epsilon(\vec{p}_i) + \frac{1}{2}\sum_{i\neq j} V(\vec{r}_i - \vec{r}_j) - \vec{E}\cdot\sum_i \vec{r}_i, \tag{B1}$$

where $\epsilon(\vec{p}_i)$ is the dispersion of the RnG electron, and $V(\vec{r}_i - \vec{r}_j)$ is the interaction between the electrons. The final term is the microscopic electric field coupling to the electron at location i in real space. Due to the nontrivial Berry curvature of the microscopic model, the spatial coordinates $\vec{r}_i$ are the gauge-invariant kinematic coordinates, $\vec{r}_i = \vec{x}_i + \vec{\mathcal{A}}(\vec{p}_i)$. This Hamiltonian is written in first-quantized notation.

The subsequent semiclassical equations of motion are

$$\dot{\vec{p}}_i = \vec{E} - \sum_{j\neq i} \vec{\nabla}_i V(\vec{r}_i - \vec{r}_j), \tag{B2}$$

$$\dot{\vec{r}}_i = \frac{\partial\epsilon}{\partial\vec{p}_i} + \dot{\vec{p}}_i \times [\mathcal{B}(\vec{p}_i)\hat{z}], \tag{B3}$$

where $\mathcal{B}$ is the Berry curvature of the microscopic RnG continuum model.

The center-of-mass momentum $\vec{p}_{\rm CM} = \sum_i \vec{p}_i$ satisfies the expected equation of motion $\dot{\vec{p}}_{\rm CM} = N\vec{E}$, where N is the total number of electrons.

The anomalous velocity contribution to the total velocity, $\vec{v}_{\rm CM}^{\,a} = \frac{1}{N}\sum_i \dot{\vec{r}}_i$, is the Berry-curvature-dependent term,

$$\vec{v}_{\rm CM}^{\,a} = \frac{1}{N}\sum_i \vec{E} \times \hat{z}\mathcal{B}(\vec{p}_i). \tag{B4}$$

This operator equation is averaged over the many-body wave function (at $\vec{E} = 0$ for linear response),

$$\langle \vec{v}_{\rm CM}^{\,a} \rangle = \vec{E} \times \hat{z}\left\langle \frac{1}{N}\sum_i \mathcal{B}(\vec{p}_i)\right\rangle \tag{B5}$$

$$= \vec{E} \times \hat{z}\left\langle \int \frac{d^2\vec{p}}{(2\pi)^2} \mathcal{B}_\alpha(\vec{p}) c_\alpha^\dagger(\vec{p}) c_\alpha(\vec{p})\right\rangle, \tag{B6}$$

where, in the second equality, we have reverted to second quantization in the noninteracting band basis in the moiré Brillouin zone, and α labels the bands of interest. This expectation value is computed within the Hartree-Fock theory, where one transforms the noninteracting fermionic operators into the Hartree-Fock basis.

[1] Y. Cao, V. Fatemi, A. Demir, S. Fang, S. L. Tomarken, J. Y. Luo, J. D. Sanchez-Yamagishi, K. Watanabe, T. Taniguchi, E. Kaxiras *et al.*, Correlated insulator behaviour at half-filling in magic-angle graphene superlattices, Nature (London) **556**, 80 (2018).

[2] Y. Cao, V. Fatemi, S. Fang, K. Watanabe, T. Taniguchi, E. Kaxiras, and P. Jarillo-Herrero, Unconventional superconductivity in magic-angle graphene superlattices, Nature (London) **556**, 43 (2018).

[3] Y.-H. Zhang, D. Mao, Y. Cao, P. Jarillo-Herrero, and T. Senthil, Nearly flat Chern bands in moiré superlattices, Phys. Rev. B **99**, 075127 (2019).

[4] F. Wu, T. Lovorn, E. Tutuc, I. Martin, and A. H. MacDonald, Topological insulators in twisted transition metal dichalcogenide homobilayers, Phys. Rev. Lett. **122**, 086402 (2019).

[5] Y.-H. Zhang, D. Mao, and T. Senthil, Twisted bilayer graphene aligned with hexagonal boron nitride: Anomalous Hall effect and a lattice model, Phys. Rev. Res. **1**, 033126 (2019).

[6] N. Bultinck, S. Chatterjee, and M. P. Zaletel, Mechanism for anomalous Hall ferromagnetism in twisted bilayer graphene, Phys. Rev. Lett. **124**, 166601 (2020).

[7] P. J. Ledwith, G. Tarnopolsky, E. Khalaf, and A. Vishwanath, Fractional Chern insulator states in twisted bilayer graphene: An analytical approach, Phys. Rev. Res. **2**, 023237 (2020).

[8] C. Repellin and T. Senthil, Chern bands of twisted bilayer graphene: Fractional Chern insulators and spin phase transition, Phys. Rev. Res. **2**, 023238 (2020).

[9] A. Abouelkomsan, Z. Liu, and E. J. Bergholtz, Particle-hole duality, emergent Fermi liquids, and fractional Chern insulators in moiré flatbands, Phys. Rev. Lett. **124**, 106803 (2020).

[10] P. Wilhelm, T. C. Lang, and A. M. Läuchli, Interplay of fractional Chern insulator and charge density wave phases in twisted bilayer graphene, Phys. Rev. B **103**, 125406 (2021).

[11] H. Yu, M. Chen, and W. Yao, Giant magnetic field from moiré induced Berry phase in homobilayer semiconductors, Natl. Sci. Rev. **7**, 12 (2020).

[12] T. Devakul, V. Crépel, Y. Zhang, and L. Fu, Magic in twisted transition metal dichalcogenide bilayers, Nat. Commun. **12**, 6730 (2021).

[13] A. L. Sharpe, E. J. Fox, A. W. Barnard, J. Finney, K. Watanabe, T. Taniguchi, M. Kastner, and D. Goldhaber-Gordon, Emergent ferromagnetism near three-quarters filling in twisted bilayer graphene, Science **365**, 605 (2019).

[14] G. Chen, A. L. Sharpe, E. J. Fox, Y.-H. Zhang, S. Wang, L. Jiang, B. Lyu, H. Li, K. Watanabe, T. Taniguchi *et al.*, Tunable correlated Chern insulator and ferromagnetism in a moiré superlattice, Nature (London) **579**, 56 (2020).

[15] M. Serlin, C. Tschirhart, H. Polshyn, Y. Zhang, J. Zhu, K. Watanabe, T. Taniguchi, L. Balents, and A. Young, Intrinsic quantized anomalous Hall effect in a moiré heterostructure, Science **367**, 900 (2020).

[16] T. Li, S. Jiang, B. Shen, Y. Zhang, L. Li, Z. Tao, T. Devakul, K. Watanabe, T. Taniguchi, L. Fu *et al.*, Quantum anomalous Hall effect from intertwined moiré bands, Nature (London) **600**, 641 (2021).

[17] B. A. Foutty, C. R. Kometter, T. Devakul, A. P. Reddy, K. Watanabe, T. Taniguchi, L. Fu, and B. E. Feldman, Mapping twist-tuned multiband topology in bilayer WSe_2, Science **384**, 343 (2024).

[18] J. Cai, E. Anderson, C. Wang, X. Zhang, X. Liu, W. Holtzmann, Y. Zhang, F. Fan, T. Taniguchi, K. Watanabe, Y. Ran, T. Cao, L. Fu, D. Xiao, W. Yao, and X. Xu, Signatures of fractional quantum anomalous Hall states in twisted $MoTe_2$, Nature (London) **622**, 63 (2023).

[19] Y. Zeng, Z. Xia, K. Kang, J. Zhu, P. Knüppel, C. Vaswani, K. Watanabe, T. Taniguchi, K. F. Mak, and J. Shan, Thermodynamic evidence of fractional Chern insulator in moiré $MoTe_2$, Nature (London) **622**, 69 (2023).

[20] H. Park, J. Cai, E. Anderson, Y. Zhang, J. Zhu, X. Liu, C. Wang, W. Holtzmann, C. Hu, Z. Liu, T. Taniguchi, K. Watanabe, J.-H. Chu, T. Cao, L. Fu, W. Yao, C.-Z. Chang, D. Cobden, D. Xiao, and X. Xu, Observation of fractionally quantized anomalous Hall effect, Nature (London) **622**, 74 (2023).

[21] F. Xu, Z. Sun, T. Jia, C. Liu, C. Xu, C. Li, Y. Gu, K. Watanabe, T. Taniguchi, B. Tong, J. Jia, Z. Shi, S. Jiang, Y. Zhang, X. Liu, and T. Li, Observation of integer and fractional quantum anomalous Hall effects in twisted bilayer $MoTe_2$, Phys. Rev. X **13**, 031037 (2023).

[22] Z. Lu, T. Han, Y. Yao, A. P. Reddy, J. Yang, J. Seo, K. Watanabe, T. Taniguchi, L. Fu, and L. Ju, Fractional quantum anomalous Hall effect in multilayer graphene, Nature (London) **626**, 759 (2024).

[23] C. Repellin, Z. Dong, Y.-H. Zhang, and T. Senthil, Ferromagnetism in narrow bands of moiré superlattices, Phys. Rev. Lett. **124**, 187601 (2020).

[24] Z. Dong, A. S. Patri, and T. Senthil, Theory of quantum anomalous Hall phases in pentalayer rhombohedral graphene moiré structures, Phys. Rev. Lett. **133**, 206502 (2024).

[25] B. Zhou, H. Yang, and Y.-H. Zhang, Fractional quantum anomalous Hall effect in rhombohedral multilayer graphene in the moiréless limit, Phys. Rev. Lett. **133**, 206504 (2024).

[26] J. Dong, T. Wang, T. Wang, T. Soejima, M. P. Zaletel, A. Vishwanath, and D. E. Parker, Anomalous Hall crystals in rhombohedral multilayer graphene. I. Interaction-driven Chern bands and fractional quantum Hall states at zero magnetic field, Phys. Rev. Lett. **133**, 206503 (2024).

[27] Z. Lu, T. Han, Y. Yao, J. Yang, J. Seo, L. Shi, S. Ye, K. Watanabe, T. Taniguchi, and L. Ju, Extended quantum anomalous Hall states in graphene/hBN moiré superlattices, arXiv:2408.10203.

[28] J. Xie, Z. Huo, X. Lu, Z. Feng, Z. Zhang, W. Wang, Q. Yang, K. Watanabe, T. Taniguchi, K. Liu *et al.*, Even-and odd-denominator fractional quantum anomalous Hall effect in graphene moire superlattices, arXiv:2405.16944.

[29] Y. H. Kwan, J. Yu, J. Herzog-Arbeitman, D. K. Efetov, N. Regnault, and B. A. Bernevig, Moiré fractional Chern insulators III: Hartree-Fock phase diagram, magic angle regime for Chern insulator states, the role of the moiré potential and goldstone gaps in rhombohedral graphene superlattices, arXiv:2312.11617.

[30] K. Huang, X. Li, S. D. Sarma, and F. Zhang, Self-consistent theory for the fractional quantum anomalous Hall effect in rhombohedral pentalayer graphene, Phys. Rev. B **110**, 115146 (2024).

[31] K. Huang, S. D. Sarma, and X. Li, Fractional quantum anomalous Hall effect in rhombohedral multilayer graphene with a strong displacement field, arXiv:2408.05139.

[32] T. Soejima, J. Dong, T. Wang, T. Wang, M. P. Zaletel, A. Vishwanath, and D. E. Parker, Anomalous Hall crystals in rhombohedral multilayer graphene. II. General mechanism and a minimal model, Phys. Rev. B **110**, 205124 (2024).

[33] Z. Dong, A. S. Patri, and T. Senthil, Stability of anomalous Hall crystals in multilayer rhombohedral graphene, Phys. Rev. B **110**, 205130 (2024).

[34] Y. Zeng, D. Guerci, V. Crépel, A. J. Millis, and J. Cano, Sublattice structure and topology in spontaneously crystallized electronic states, Phys. Rev. Lett. **132**, 236601 (2024).

[35] T. Tan and T. Devakul, Parent Berry curvature and the ideal anomalous Hall crystal, Phys. Rev. X **14**, 041040 (2024).

[36] D. Waters, A. Okounkova, R. Su, B. Zhou, J. Yao, K. Watanabe, T. Taniguchi, X. Xu, Y.-H. Zhang, J. Folk, and M. Yankowitz, Interplay of electronic crystals with integer and fractional Chern insulators in moiré pentalayer graphene, arXiv:2408.10133.

[37] S. Musser, M. Cheng, and T. Senthil, Fractionalization as an alternate to charge ordering in electronic insulators, arXiv:2408.03984.

[38] Related charge-ordered states at specific commensurate fillings which show an integer quantum Hall effect have been discussed in the name of "generalized anomalous Hall crystals" or "topological charge density waves"; see Ref. [52], and references therein.

[39] If we allow multiple electrons per CDW unit cell, then the fillings can be $\frac{p}{m^2+n^2+mn}$ with $m, n, p \in \mathbb{Z}$, which can fall into the regime of $\frac{1}{2} < \nu < 1$. We note that for $p = m^2 + n^2 + mn - 1$, this is the same as the hole crystal, where holes form a triangular lattice commensurate with moiré, with one hole per CDW unit cell. However, it is energetically unlikely that a crystal state in a continuum system has multiple electrons per unit cell.

[40] G. Gruner, *Density Waves in Solids* (CRC Press, Boca Raton, FL, 2018).

[41] D. S. Fisher, Collective transport in random media: From superconductors to earthquakes, Phys. Rep. **301**, 113 (1998).

[42] S. Brazovskii and T. Nattermann, Pinning and sliding of driven elastic systems: From domain walls to charge density waves, Adv. Phys. **53**, 177 (2004).

[43] C. O. Reichhardt, Depinning and nonequilibrium dynamic phases of particle assemblies driven over random and ordered substrates: A review, Rep. Prog. Phys. **80**, 026501 (2017).

[44] Recall our assumption that we ignore any anomalous velocity of the hole crystal.

[45] This does not violate the statement—known as Bloch's second theorem—that typically equilibrium many-body states will have zero electric current. A sophisticated discussion of a loophole to Bloch's second theorem is in Ref. [53], and this loophole applies to chiral quantum Hall edge states (see, also, Ref. [54]).

[46] X.-Y. Song, Y.-H. Zhang, and T. Senthil, Phase transitions out of quantum Hall states in moiré materials, Phys. Rev. B **109**, 085143 (2024).

[47] Andrea F. Young (private communication).

[48] S. D. Sarma and M. Xie, Thermal crossover from a Chern insulator to a fractional Chern insulator in pentalayer graphene, Phys. Rev. B **110**, 155148 (2024).

[49] G. Shavit, Entropy-enhanced fractional quantum anomalous Hall effect, Phys. Rev. B **110**, L201406 (2024).

[50] Z. Wei, A.-K. Wu, M. Gonçalves, and S.-Z. Lin, Edge-driven transition between extended quantum anomalous Hall crystal and fractional Chern insulator in rhombohedral graphene multilayers, arXiv:2409.05043.

[51] K. Huang, S. D. Sarma, and X. Li, Impurity-induced thermal crossover in fractional Chern insulators, arXiv:2409.04349.

[52] R. Su, D. Waters, B. Zhou, K. Watanabe, T. Taniguchi, Y.-H. Zhang, M. Yankowitz, and J. Folk, Generalized anomalous Hall crystals in twisted bilayer-trilayer graphene, arXiv:2406.17766.

[53] D. V. Else and T. Senthil, Critical drag as a mechanism for resistivity, Phys. Rev. B **104**, 205132 (2021).

[54] A. Kapustin and L. Spodyneiko, Absence of energy currents in an equilibrium state and chiral anomalies, Phys. Rev. Lett. **123**, 060601 (2019).